International Journal for Modern Trends in Science and Technology, 8(09): 221-230, 2022

ISSN: 2455-3778 online
DOI: https://doi.org/10.46501/IJMTST0809046
Available online at: http://www.ijmtst.com/vol8issue09.html

Three-Phase Solar PV Design with Integrated UPQC and Performance Monitering by ANN

Malapati Ratnakar[1] | Dr. M Vasavi Uma Maheswari[2]

[1]PG Scholar, Department of EEE, Acharya Nagarjuna University, Guntur, India.
[2]Assistant Professor, Department of EEE, Acharya Nagarjuna University, Guntur, India.
Corresponding Author : mahi_vasavi1@yahoo.co.in

To Cite this Article
Malapati Ratnakar and Dr. M Vasavi Uma Maheswari. Three-Phase Solar PV Design with Integrated UPQC and Performance Monitering by ANN. International Journal for Modern Trends in Science and Technology 2022, 8(09), pp. 221-230. https://doi.org/10.46501/IJMTST0809046

Article Info
Received: 30 August 2022; Accepted: 17 September 2022; Published: 21 September 2022.

ABSTRACT

The design of a three-phase solar PV system with the integrated UPQC, an analysis of its performance and control operations of UPQC byadopting an artificial intelligence(ANN) are discussed in this paper. The basic components of PV-UPQC are shunt and series voltage compensators that are connected in series and parallel by a single DC link. Shunt compensator is meant to evoke the power from PV array and also compensate the load current harmonics. Moving average filter (MAF) enhanced the system performance and improving synchronous reference frame control. The series voltage compensator is meant to compensate grid-side power quality issues like voltage sags and swells. It injects the voltage in-phase or out-of-phase of the grid appropriately. The main benefits due to this proposed system is to clean energy generation and improving power quality. The MATLAB Simulink is used to assess the system's performance in both steady state and dynamic conditions. The primary focuses isto implement an ANN (Artificial Neural Network) rather than a PI controller for better performance and minimize THD issues at various conditions of irradiance, PCC voltage sag/swell, and load unbalancing. ANN will yield the best results and enhance power quality.

.

KEYWORDS: Power quality, Solar power, Shunt compensator, Series compensator, MPPT, and ANN.

1. INTRODUCTION

The penetration of power electronic loads has increased with the development of semiconductor technology. These loads, which are efficient, but draw non-linear currents. Those non linear loads are computer power supplies, variable speed drives, switched mode power supplies, etc. At the point of common coupling (PCC) in distribution systems, these nonlinear currents may result in voltage distortion. The benefit of using PV as a source of energy is that small buildings and apartments can generate clean energy through the installation of rooftop and solar tree PV systems [1],[2]. The installation of rooftop PV systems in residential and small commercial buildings is done for the purpose of accentuating the production of clean energy. Especially in the ineffective distribution systemsleads to voltage issues such voltage sags and swells [3, 4] and will increase the penetration of such a system because the PV supply is intermittent. These voltage quality problems cause the electronic devices and systems to

frequently trip falsely, increase the temperature of the capacitor banks [8], [10], and snag or falsely trigger the electronic systems. Due to these challenges, there are significant power quality issues on both the load side and the grid side of current distribution networks.Due to the demand for clean energy generation and indeed the best quality of power needed by complex electronic loads, it is necessary to have a system that can execute many tasks simultaneously, i.e., that can produce clean energy while also enhancing the power quality. In [11],[12] explained about the uses of three phase multi-functional conversion of solar energy system to compensate for load and grid side power quality concerns. Even though it has the ability to regulate load voltage and is at the root of injecting reactive power, a single phase solar PV inverter with active filter capabilities integrates clean energy generation with active filtering. But it is unable to both maintain and manage PCC voltage and utility factor at the grid's current continuously. Recent proposals for series active filters [15],[16] have been made in response to the demanding power quality requirements for complex electronics loads. Compared to shunt active filter and series active power filter, unified power quality conditioner(UPQC) have both series and shunt compensators, it is performing the both load voltage regulation and maintaining grid current sinusoidal at unity power factor. A solar photovoltaic system integrated with the dynamic voltage restorer has been proposed in [17]. PV array integration with UPQC has been suggested in [18]–[20]. An embedded UPQC to PV array has various benefits over typical grid-connected inverters, including enhancing the grid's power quality.Along with improving the converter's ability,the ride through faults during transient conditions, it shields the crucial loads from grid-side disturbances.

The generation of reference signals is a significant responsibility in the PV-UPQC control operation, with signal strategies split into time domain and frequency domain procedures [8]. The time domain strategy is more often utilized in execution because it reduces the processing applications. The most frequently applied methodologies are reactive power theory (p-q theory), synchronous reference frame theory (d-q theory), and instantaneous symmetrical component theory [23]. When the reference frame theory is employed in an unbalanced condition, a double periodic element is introduced in the d-axis current. As a reason, use a low pass filter with a very low cutoff frequency to remove the double harmonic currents [24]. In this procedure, the d-axis current is filtered to produce the primary load active current. It will provide the converter with optimal attenuation, and without diminishing bandwidth [25]. In [26],[27], moving average filter (MAF) was employed to boost the efficiency of DC-link controllers as well as revised utilizing phase locked loop (PLL). The great benefit of using ANN to drive PV-UPQC instead of pi controllers is that it reduces THD (total harmonic distortion) and grid current fluctuations.The entire research will address the design and performance analysis of three phase PV-UPQC utilizing an ANN controller. To boost performance characteristics during load active current recovery, a MAF-based d-q theory-based control was adopted.

2. SYSTEM CONFIGURATION AND DESIGN

Figure 1 illustrates the three-phase PV-UPQC configuration. The PV-UPQC is constituted of a shunt and a series compensator linked by a single DC-link. The shunt compensator is connected to load side, while series compensator is connected to the grid. Solar PV is connected directly to the UPQC DC network via a reverse blocking diode. The series compensator compensates for grid voltage sags/swells while operating in voltage control mode. Interfacing inductors interface the shunt and series compensators to the grid. The voltage generated by the series compensator is injected into the grid via a series injection transformer. Harmonics are generated by converter switching activity and filtered by using Ripple filters. A bridge rectifier is composed of a nonlinear load and a voltage-fed load.

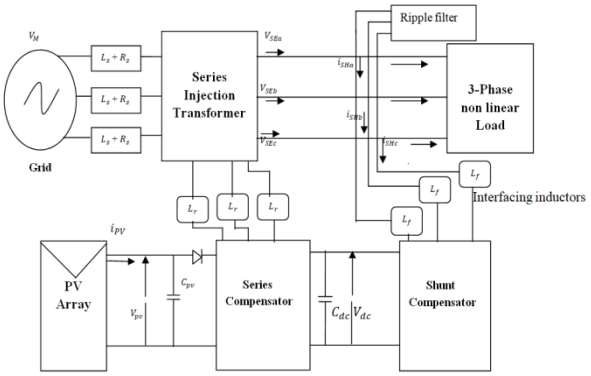

Fig.1. System Configuration of PV-UPQC

A. Design of PV-UPQC

The design techniques involve proper sizing of the PV array, DC link capacitor, DC link voltage level, etc. The shunt compensator is calibrated to withstand the peak output from the PV array, as well as compensates the load current, reactive power and current harmonics. The PV array is integrated directly to the DC connection, and it is sized so that the MPP voltage is identical to the required DC link voltage. Under normal conditions, the PV array provides load active power together with grid power. Other design elements include a series injection transformer, interface inductors, and series and shunt compensators. The PV-UPQC design is discussed below.

1)*Voltage magnitude of DC link:* The magnitude of the DC link voltage has always been determined by the depth of modulation and the system's per-phase voltage. The magnitude of the DC link voltage should be more than double peak per-phase voltage of a three-phase system [8] and is expressed as,

$$V_{dc}=\frac{2\sqrt{2}V_{LL}}{\sqrt{3}m}(1)$$

where m is the depth of modulation and . $V_{LL}$is the grid line voltage. The line voltage is 415V, and the DC-bus voltage must be at least 677.7V. The DC bus voltage is around 700V, which is the same as or equal to the MPPT working voltage of the PV array under STC circumstances.

2) DC-Bus Capacitor Rating: The rating is determined by the amount of power required as well as the Dc-bus voltage level. The DC-Bus capacitor rating of energy balance equation is as follows:

$$C_{dc}=\frac{3kaV_{ph}I_{sh}}{0.5\times(V_{dc}^2-V_{dc\,1}^2)}$$

$$=\frac{3\times0.1\times1.5\times239.6\times34.5\times0.03}{0.5\times(700^2-677.79^2)}$$

$$=9.3\text{mF} \quad (2)$$

where V_{dc} is the average DC-bus voltage, V_{dc1} is the lowest required value of DC-bus voltage, a is the overloading factor, V_{ph} is per-phase voltage, t is the minimum time required for attaining steady value after a disturbance, Ish is per-phase current of shunt compensator, k factor considers variation in energy during dynamics.

According to (2), the minimum needed DC-link voltage is V_{dc1} = 677.69 V, V_{dc} = 700 V, V_{ph}= 239.60 V, I_{sh}=57.5 A, t= 30 ms, a = 1.2, and for dynamic energy change = 10%, k= 0.1, the value of C_{dc}= 9.3 mF.

3) *Interface Inductor for Shunt Compensator*: The shunt compensator's interfacing inductor rating is established by that of the ripple current, switching frequency, and DC link voltage. The interfacing inductor rating is expressed as,

$$L_f=\frac{\sqrt{3}mV_{dc}}{12af_{sh}I_{cr,pp}}=\frac{\sqrt{3}\times1\times700}{12\times1.2\times10000\times6.9}$$

$$=800\mu\text{H}\approx1\text{mH} \quad (3)$$

where m is the modulation depth, a is pu value of maximum overload, f_{sh} is the switching frequency, $I_{cr,pp}$ is the ripple current of inductor which is taken as 20% of rms phase current of shunt compensator. With m=1, a=1.2,f_{sh}=10KHz and V_{dc}=700V one obtain800μH which is roughly at 1mH.

4) *Series Injection Transformer*:-: The PV-UPQC is intended to compensate for a 0.3 pu sag/swell, i.e. 71.88 V As a result, the needed voltage for injection is roughly 71.88 V, offeringwhen the series compensator has a low modulation index. The voltage across the DC-link is 700V. In order to run the series,One maintains modulation by using a compensator with the minimum harmonics.The series compensator's index is close to unity as a result, a series transformer with a turns ratio is expressed as

$$K_{SE}=\frac{V_{vsc}}{V_{SE}}=3.33\approx3(4)$$

K_{SE} is 3.33. the rating of series injected transformer rating is

$$S_{SE}=3V_{SE}I_{SE\,sag}=3\times72\times46=10\text{KVA} \quad (5)$$

The current flowing through the series VSC is the same as the current flowing through the grid.

The supply current is 46 A under sag conditions of 0.3 pu, resulting in a VA rating of 10KVA for the injection transformer.

5) Interfacing Inductor of Series Compensator: The series compensator interfacing inductor rating is depends upon the ripple current bat the swell condition, switching frequency and DC link voltage. Its rating is given as,

$$L_r=\frac{\sqrt{3}\times mV_{dc}K_{SE}}{12af_{se}I_r}=\frac{\sqrt{3}\times1\times700\times3}{12\times1.2\times10000\times7.1}$$

$$=3.6\text{mH} \quad (6)$$

where m is the modulation depth, a is the pu value of the maximum overload, f_{se} is the switching frequency ,I_r is the ripple current of the inductor, which is taken as 20% of the grid current. Here m=1, a=1.2, f_{se}=10KHz,

V_{dc} =700V and 20% ripple current, one gets 3.6mH as selected value

3. CONTROLOF PV-UPQC

The PV-UPQC consists of shunt and series voltage compensator sub systems. The shunt compensator is deployed as a compensate for load power quality issues such as load harmonic currents and load reactive power. The shunt compensator in the PV-UPQC performs an additional role in this study, which is to collect power from the PV-array using an MPPT (maximum power point tracking) algorithm. on the other hand, the series compensator, is used to protect the load from grid-side power quality concerns such as voltage sags/swells by injecting suitable voltage in-phase with the grid.

A) Control of Shunt Compensator

By utilizing an MPP, the shunt compensator obtains the maximum power from the solar PV-array. The reference voltage was established by the MPPT algorithm for the PV-UPQC DC-link. MPPT algorithms that are regularly used [28] include the Perturb and Observe (P& O) algorithm and the incremental conductance algorithm (INC). The (P& O) algorithm is applied in this study to implement MPPT. A PI-controller is used to keep the DC-link voltage at the generated reference. For getting better compensation and reducing the load currents an ANN controller is used instead of a PI controller this paper.An ANN controller which is the find out errors through weight adjustment.The shunt compensator collects the active fundamental component of the load current to perform load current compensation. The shunt compensator is managed in this paper by extracting the fundamental active component of the load current using the SRF methodology. Figure 2 illustrates the shunt compensator's control structure with the ANN.The voltages at the load is compared with reference voltages is given as input layer of ANN. The designed ANN controller has 3 layers composed of 2 input layers. 2 hidden layers and 1 output layer. After complete training of ANN the output produced in real and reactive. Using the phase and frequency information collected from the PLL, the load currents are switched to the d-q-0 domain. The PCC voltage is fed into the PLL. The load current's d-component (ILd) is filtered to isolate the DC component (ILdf), which constitutes the basic component in the abc reference frame. A moving average filter (MAF) is used to recover the DC component without deteriorating the dynamic performance. The moving average filter's transfer function is expressed as,

$$\text{MAF(s)}=\frac{1-e^{-T_w s}}{T_w s} \quad (7)$$

here T_w is the moving average filter window length. As the lowest harmonic present in the d-axis current is double harmonic component, T_w is kept at half of fundamental time period. The MAF unity gain and zero gain integer multiples of window length. T_w denotes the length of the moving average filter window. T_w is preserved at half of the fundamental time period because the lowest harmonic present in the d-axis current is a double harmonic component. MAF integer multiples of window length with unity gain and zero gain.The equivalent current component due to PV array is,

$$I_{PVg} = \frac{2}{3}\frac{P_{pv}}{V_s} \quad (8)$$

where P_{pv} power of PV-array and V_s is the magnitude of the voltage at PCC. The reference grid current is,

$$I_{sd}^{*}=I_{Ldf} + I_{loss} - I_{pvg} \quad (9)$$

Here I_{sd}^{*} is converted to the abc domain reference grid currents. In a hysteresis current controller the reference grid currents are compared with sensed grid currents to generate the gating pulses for shunt converter.

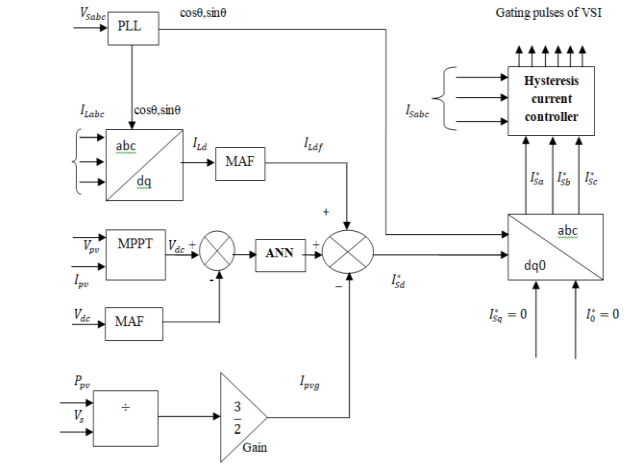

Fig.2. Control Structure of Shunt Compensator

B. Control of Series Compensator:

Pre-sag compensation, in-phase compensation, and energy optimal compensation are the series compensator control techniques. [29],[30] provide a full overview of series compensator control techniques. The series compensator injects voltage into the grid

in-phase, resulting in the minimal voltage injected by the compensator. Figure 3depicts the control structure of a series compensator with the controllers of PI and also ANN. The reference load voltage is generated by PCC utilizing the phase and frequency information provided from PLL. PLL is used to extract the fundamental component of PCC voltage, and this PLL generates the reference axis in the d-q-0 domain.PCC and load voltages are changed as the d-q-o domain. The reference load voltage is in phase with the PCC voltages; the peak reference load voltage is the load reference voltage's d-axis element value. The q-axis component remains at zero. The difference between the load reference voltage and the PCC voltage is used to compute the reference voltage for the series compensator. The actual series compensator voltages are determined by subtracting the load voltage from the PCC voltages. The ANN controllers use the difference between the actual series compensator and reference voltages to produce the required reference signals.The output of ANN controller is the reference variable for the PWM generator. Therefore, the output of ANN with varying amplitude and phase passes through a comparator and is compared with a carrier signal. When the ANN output's magnitude is more than carrier signal's magnitude, the PWM circuit generates high output and when the ANN output's magnitude is less than carrier signal's magnitude, the PWM circuit produces low output.These reference signals are turned into the abc domain and fed via the pulse width modulation (PWM) voltage controller, to provide appropriate gating signals for the series compensators VSC.

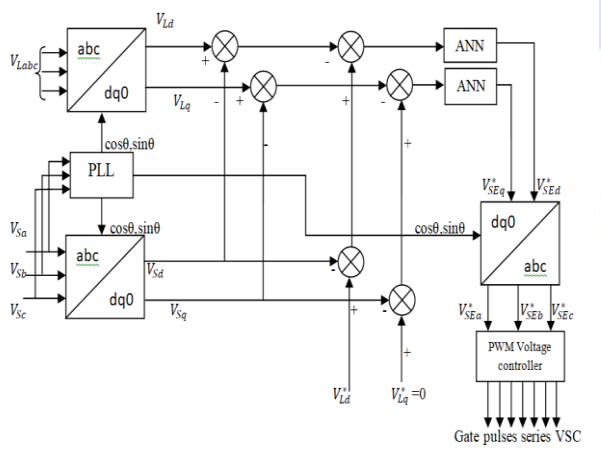

Fig.3. Control Structure of Series Compensator.

4. SIMULATION STUDIES

The steady-state and dynamic performances of PV-UPQC are evaluated by using Matlab-Simulink software. As a three phase non linear load with R load, a three phase bridge rectifier is employed. For the simulation, the solver step size is 1e-6s. The system is exposed to a wide range of dynamic circumstances, including sag and swell variations in PCC voltage load unbalancing condition and PV irradiation.

A).Performance of PV-UPQC at PCC Voltage Fluctuations

Figure 4(a,b) demonstrates the dynamic performance of PV-UPQC in situations of PCC voltage sags/swells. The irradiance (G) is kept constant at 1000W/m2. PCC voltages (V_s), load voltages (V_L), series compensator voltages (V_{SE}), DC-link voltage (V_{dc}), solar PV array current (I_{pv}), solar PV array power (P_{pv}, grid currents (I_s), load currents (I_{La}, I_{Lb}, I_{Lc}), shunt compensator currents include the several observed signals (I_{SHa}, I_{SHb}, I_{SHc}).V_{Sab} falls to 170 V and increases to 270 V during PCC voltage sag. To keep V_{Lab} at 220 V, the series compensator injects voltage that is in phase or out of phase with respect to the PCC voltage. I_{Sa} Increases during voltage sag conditions.While I_{Sa} drops during voltage swell conditions, to preserve the system's power balance.Voltage sag is 0.3pu between 0.7s and 0.75s, and voltage swell is 0.3pu between 0.8s and 0.85s. Under these instances, the series compensator compensated for the grid voltage by injecting a suitable voltage V_{SE} in reverse polarity with the grid voltage disturbance to sustain the load voltage at the maximum voltage condition.

Fig.4(a,). Performance of PV-UPQC under Voltage sag/swell condition.with PI controller

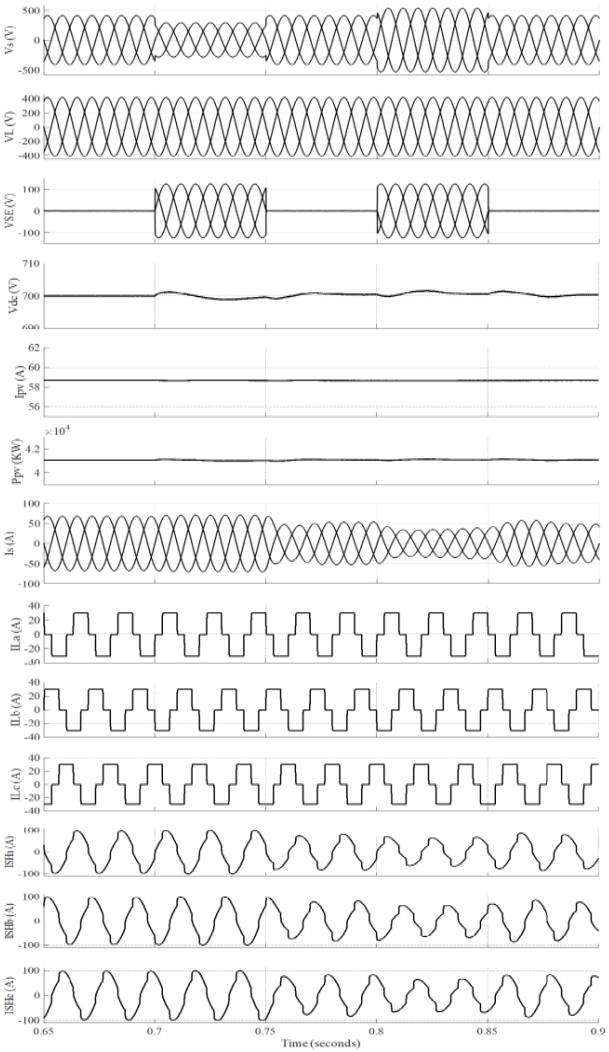

Fig.4(b). Performance of PV-UPQC under Voltage sag/swell condition.with ANN controller

B. Performance of PV-UPQC at Load Unbalancing Condition

Figure 5(a,b) illustrates the dynamic performance of PV-UPQC during load imbalanced conditions. The load's phase 'b' is disconnected at t=0.8s. It can be seen that the grid current is sinusoidal and has a unity power factor . The current delivered into the grid increases as the total effective loadfalls. The DC-link voltage is similarly stable, remaining close to the ideal regulated value of 700 V. Even when the load is asymmetrical, the grid current remains sinusoidal. The current of the shunt compensator combination of active current from PV array and load current harmonics. The DC-link voltage V_{dc} is set to the desired value. Because there is more surplus PV power available to be fed into PCC due to the general drop in load power under unbalanced load conditions, I_{Sab} increases.

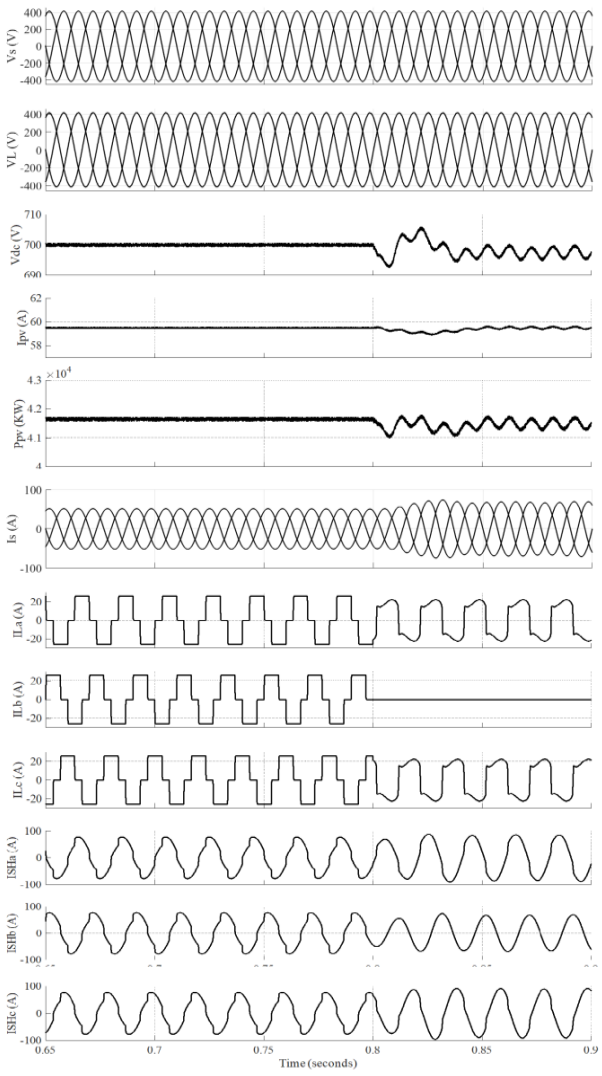

Fig. 5(a).. Performance PV-UPQC during Load Unbalance Condition with Pi Controller.

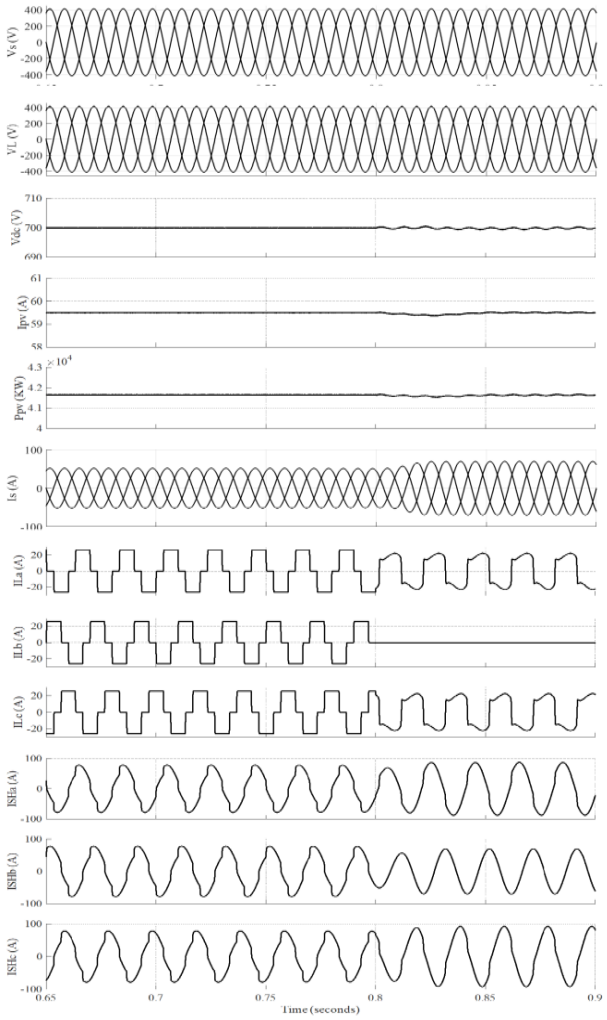

Fig. 5(b).. Performance PV-UPQC during Load Unbalance Condition with ANN Controller.

C. Performance of PV-UPQC under Varying Irradiation:-The dynamic performance of PV-UPQC at solar irradiation is demonstrated in Fig.6. The irradiance is increased gradually from 500W/m2 at 0.8s to 1000W/m2 at 0.85s. It is observedthat as irradiation rises, so does the output of the PV array as a result of the PV array feeding power into the grid, grid current increasesinside the grid .An MPPT is regulated by the shunt compensator iscompensating for harmonics caused by load current.Compensating for harmonics caused by load current. Figures.7 demonstrate harmonic spectrum, load current, and grid current. It has been discovered that the load current THD is 29.49%, and the grid current THD is 2.04%.. The controller PI demonstrates the THD. The PV-UPQC reaction during a change in solar irradiation intensity is depicted in Fig.6 V_{pv}, I_{pv}, I_{SHb}, and I_{Sb} waveforms were collected. The photovoltaic (PV) irradiation is raised from 500W/m2 to 1000W/m2. It can be seen that when irradiation grows, also the available the PV array power, which raises the shunt compensator current and, as a result, the current sent into the grid. Table.1 illustrates the during the other intermediate irradiation circumstances, It shows the MPPT efficiency as well as other parameters. The system can track MPPT with an effectiveness of more than 99% under all irradiation conditions.

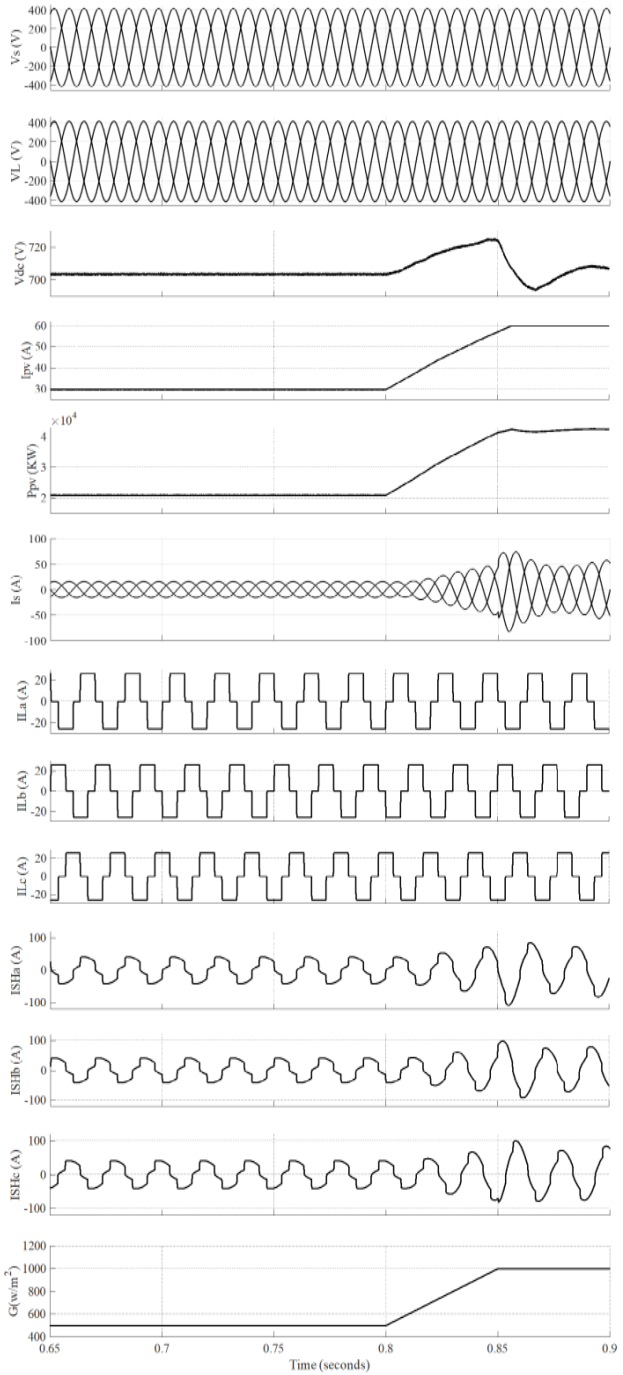

Fig. 6(a). Performance PV-UPQC at Varying Irradiation Condition with PI controller

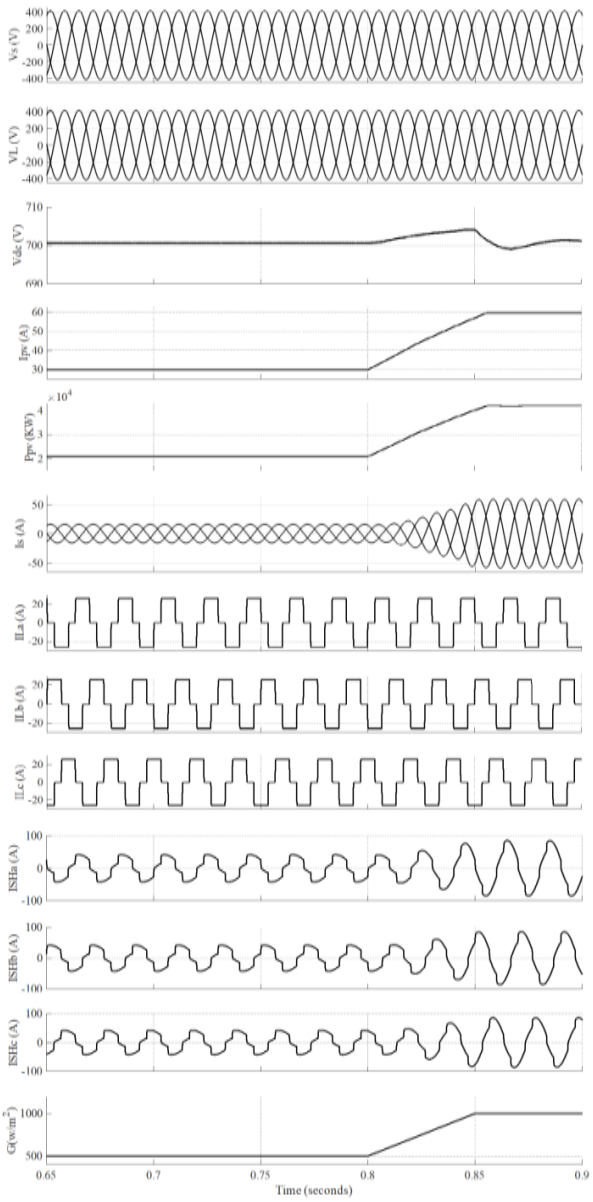

Fig. 6(b). Performance PV-UPQC at Varying Irradiation Condition with ANN controller.

Figures 7(a,b) demonstrate harmonic spectrum, load current, and grid current. It has been discovered that the load current THD is 29.44%, and the grid THD is 0.38%.. The controller ANN demonstrates the THD. An ANN compared to PI controller THD value of grid current is decreased That is illustrated in fig 8(a,b). and it gave better results in the irradiance conditions also fastest response at the fault conditions. The main benefit by adapting the ANN controller to minimizes the THD as much as possible with non linear currents are present in the load side.

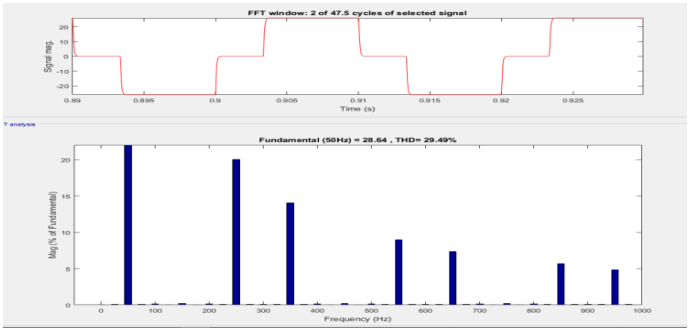

Fig. 7(a). Load Current Harmonic Spectrum and THD with PI controller

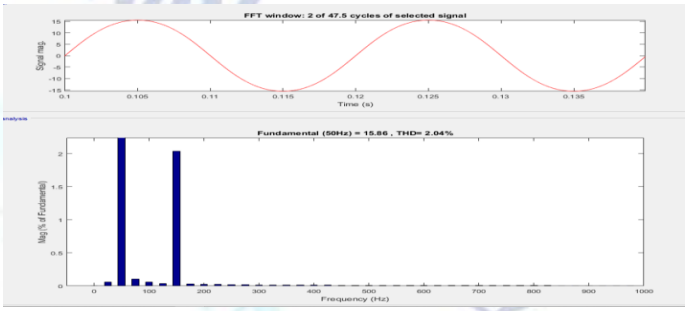

Fig. 7(b). Grid Current Harmonic Spectrum and THD with PI controller

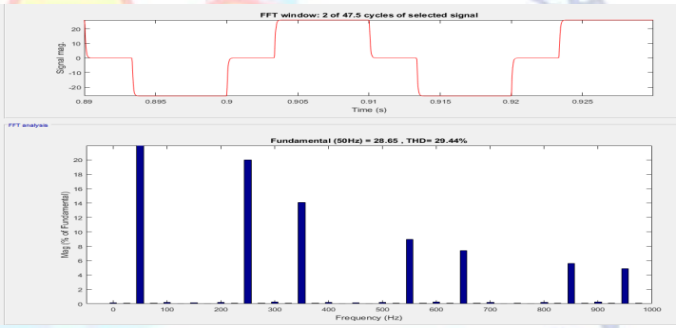

Fig. 8(a). Load Current Harmonic Spectrum and THD with ANN controller

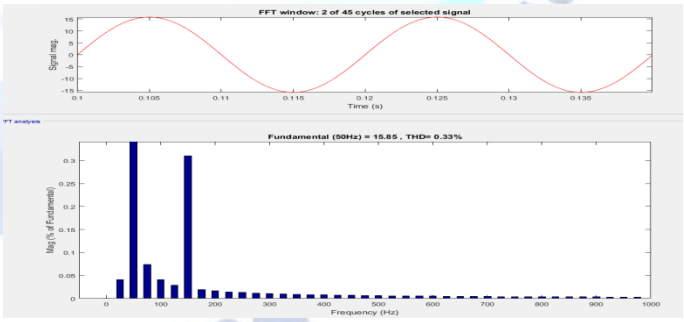

Fig. 8(b) Grid Current Harmonic Spectrum and THD with ANN controller

5. CONCLUSION

Considering irregular irradiation and grid voltage sags/swells, the design and dynamic performance of three-phase PVUPQC were evaluated. The system's performance has been proven through experimentation on a scaled-down laboratory version. PVUPQC is reported to reduce harmonics induced by nonlinear

load andkeeps grid current THD under IEEE-519 limitsstandard. The system is determined to be stable under a wide range of conditions, Irradiation, voltage sags/swell, and load unbalance are all factors to consider. The performance of d-q control, particularly when the load is unbalanced.has been enhanced by the addition of a moving average filter(MAF) can be performing with PV-UPQC is an excellent modern option. Finally combining distributed generation and dissemination enhancement of power quality by using ANN controller, for fast response as well as better results in the PV power while the dynamic performance.

Table: 1

Comparison of PI with ANN with respected to FFT values (THD %)

Controller	PI controller	ANN controller
Source current (I_S)	2.04%	0.38%
Load current (I_L)	29.52%	29.44%

Conflict of interest statement

Authors declare that they do not have any conflict of interest.

REFERENCES

[1] B. Mountain and P. Szuster, "Solar, solar everywhere: Opportunities and challenges for Australia's rooftop pv systems," IEEE Power and Energy Magazine, vol. 13, no. 4, pp. 53–60, July 2015.

[2] A. R. Malekpour, A. Pahwa, A. Malekpour, and B. Natarajan, "Hierarchical architecture for integration of rooftop pv in smart distribution systems," IEEE Transactions on Smart Grid, vol. PP, no. 99, pp. 1–1, 2017.

[3] Y. Yang, P. Enjeti, F. Blaabjerg, and H. Wang, "Wide-scale adoption of photovoltaic energy: Grid code modifications are explored in the distribution grid," IEEE Ind. Appl. Mag., vol. 21, no. 5, pp. 21–31, Sept 2015.

[4] M. J. E. Alam, K. M. Muttaqi, and D. Sutanto, "An approach for online assessment of rooftop solar pv impacts on low-voltage distribution networks," IEEE Transactions on Sustainable Energy, vol. 5, no. 2, pp. 663–672, April 2014.

[5] J. Jayachandran and R. M. Sachithanandam, "Neural network-based control algorithm for DSTATCOM under nonideal source voltage and varying load conditions," Canadian Journal of Electrical and Computer Engineering, vol. 38, no. 4, pp. 307–317, Fall 2015.

[6] A. Parchure, S. J. Tyler, M. A. Peskin, K. Rahimi, R. P. Broadwater, and M. Dilek, "Investigating pv generation induced voltage volatility for customers sharing a distribution service transformer," IEEE Trans. Ind. Appl., vol. 53, no. 1, pp. 71–79, Jan 2017.

[7] E. Yao, P. Samadi, V. W. S. Wong, and R. Schober, "Residential demand side management under high penetration of rooftop photovoltaic units," IEEE Transactions on Smart Grid, vol. 7, no. 3, pp. 1597–1608, May 2016.

[8] B. Singh, A. Chandra and K. A. Haddad, Power Quality: Problems and Mitigation Techniques. London: Wiley, 2015.

[9] M. Bollen and I. Guo, Signal Processing of Power Quality Disturbances. Hoboken: John Wiley, 2006.

[10] P. Jayaprakash, B. Singh, D. Kothari, A. Chandra, and K. Al-Haddad, "Control of reduced-rating dynamic voltage restorer with a battery energy storage system," IEEE Trans. Ind. Appl., vol. 50, no. 2, pp. 1295– 1303, March 2014.

[11] B. Singh, C. Jain, and S. Goel, "ILST control algorithm of single stage dual purpose grid connected solar pv system," IEEE Trans. Power Electron., vol. 29, no. 10, pp. 5347–5357, Oct 2014.

[12] R. K. Agarwal, I. Husain, and B. Singh, "Three-phase single-stage grid tied solar pvecs using PLL-less fast CTF control technique," IET Power Electronics, vol. 10, no. 2, pp. 178–188, 2017.

[13] Y. Singh, I. Husain, B. Singh, and S. Mishra, "Single-phase solar grid interfaced system with active filtering using adaptive linear combiner filter-based control scheme," IET Generation, Transmission Distribution, vol. 11, no. 8, pp. 1976–1984, 2017.

[14] T.-F. Wu, H.-S. Nien, C.-L. Shen, and T.-M. Chen, "A single-phase inverter system for pv power injection and active power filtering with nonlinear inductor consideration," IEEE Trans. Ind. Appl., vol. 41, no. 4, pp. 1075–1083, July 2005.

[15] A. Javadi, A. Hamadi, L. Woodward, and K. Al-Haddad, "Experimental investigation on a hybrid series active power compensator to improve power quality of typical households," IEEE Trans. Ind. Electron., vol. 63, no. 8, pp. 4849–4859, Aug 2016.

[16] A. Javadi, L. Woodward, and K. Al-Haddad, "Real-time implementation of a three-phase these based on vsc and p+r controller to improve power quality of weak distribution systems," IEEE Transactions on Power Electronics, vol. PP, no. 99, pp. 1–1, 2017.

[17] A. M. Rauf and V. Khadkikar, "Integrated photovoltaic and dynamic voltage restorer system configuration," IEEE Transactions on Sustainable Energy, vol. 6, no. 2, pp. 400–410, April 2015.

[18] S. Devassy and B. Singh, "Design and performance analysis of three phase solar pv integrated upqc," in 2016 IEEE 6th International Conference on Power Systems (ICPS), March 2016, pp. 1–6.

[19] K. Palanisamy, D. Kothari, M. K. Mishra, S. Meikandashivam, and I. J. Raglend, "Effective utilization of unified power quality conditioner for interconnecting PV modules with grid using power angle control method," International Journal of Electrical Power and Energy Systems, vol. 48, pp. 131 – 138, 2013.

[20] S. Devassy and B. Singh, "Modified p-q theory based control of solar pv integrated upqc-s," IEEE Trans. Ind. Appl., vol. PP, no. 99, pp. 1–1, 2017.

[21] S. K. Khadem, M. Basu, and M. F. Conlon, "Intelligent islanding and seamless reconnection technique for micro grid with upqc," IEEE Journal of Emerging and Selected Topics in Power Electronics, vol. 3, no. 2, pp. 483–492, June 2015.

[22] J. M. Guerrero, P. C. Loh, T. L. Lee, and M. Chandorkar, "Advanced control architectures for intelligent micro grids; part ii: Power quality, energy storage, and ac/dc micro grids," IEEE Transactions on Industrial Electronics, vol. 60, no. 4, pp. 1263–1270, April 2013.

[23] B. Singh and J. Solanki, "A comparison of control algorithms for dstatcom ," IEEE Transactions on Industrial Electronics, vol. 56, no. 7, pp. 2738–2745, July 2009.

[24] B. Singh, C. Jain, S. Goel, A. Chandra, and K. Al-Haddad, "A multifunctional grid-tied solar energy conversion system with anf-based control approach," IEEE Transactions on Industry Applications, vol. 52, no. 5, pp. 3663–3672, Sept 2016.

[25] S. Golestan, M. Ramezani, J. M. Guerrero, and M. Monfared, "dq-frame cascaded delayed signal cancellation- based pll: Analysis, design, and comparison with moving average filter-based pll," IEEE Transactions on Power Electronics, vol. 30, no. 3, pp. 1618–1632, March 2015.

[26] R. Pea-Alzola, D. Campos-Gaona, P. F. Ksiazek, and M. Ordonez, "Dclink control filtering options for torque ripple reduction in low-power wind turbines," IEEE Trans. Power Electron., vol. 32, no. 6, pp. 4812– 4826, June 2017.

[27] S. Golestan, M. Ramezani, J. M. Guerrero, F. D. Freijedo, and M. Monfared, "Moving average filter based phase-locked loops: Performance analysis anddesign guidelines," IEEE Trans. Power Electron., vol. 29, no. 6, pp. 2750–2763, June 2014.

[28] B. Subudhi and R. Pradhan, "A comparative study on maximum power point tracking techniques for photovoltaic power systems," IEEE Transactions on Sustainable Energy, vol. 4, no. 1, pp. 89–98, Jan 2013.

[29] A. Sadigh and K. Smedley, "Review of voltage compensation methods in dynamic voltage restorer DVR," in IEEE Power and Energy Society General Meeting, July 2012, pp. 1–8.

[30] A. Rauf and V. Khadkikar, "An enhanced voltage sag compensation scheme for dynamic voltage restorer," IEEE Trans. Ind. Electron., vol. 62, no. 5, pp. 2683–2692, May 2015.

[31] "IEEE recommended practices and requirements for harmonic control in electrical power systems," IEEE Std 519-1992, pp. 1–112, April 1993